International Journal of Computational Bioinformatics and In Silico Modeling
Vol. 3, No. 5 (2014): 497-501
Research Article
Open Access

ISSN: 2320-0634

In Silico Screening for Novel Inhibitors of Invasion Protein Antigen IpaD of *Shigella flexneri* - an agent of Shigellosis

Md. Jahangir Alam and Tithi Roy*

Department of Genetic Engineering and Biotechnology, Shahjalal University of Science and Technology, Sylhet 3114; Bangladesh

*Corresponding author: Roy Tithi; e-mail: tithiroy33@student.sust.edu

Received: 24 August 2014 Accepted: 18 September 2014 Online: 27 September 2014

ABSTRACT

Shigellosis is a most common disease of developing to industrialized countries with its most spreadable, contractable agent *Shigella flexneri*. It uses type three secretion system for invasion composed of a needle, and a needle tip protein ipaD which is responsible for the proper translocation of ipaB/ipaC complex forming a pore on the host cell membrane, causing host cell apoptosis. The ipaD is a potential drug target for shigellosis; this study has carried out by fixed-protein flexible-ligand based screening for inhibitor design. Protein model was built using Modeller and mutual interaction between protein and ligand was evaluated using AutoDockVina. Five potential ligands analyzed for each of the three active site of this needle-tip protein. Analyzing the binding energy, physicochemical properties and interaction pattern, ZINC13298260 and ZINC34037183 are considerably two good inhibitors. This theorized study proposes these ligands as potential therapeutics against shigellosis.

Keywords: TTSS; ipaD; homology modeling; fixed-protein flexible ligand docking; docking

INTRODUCTION

Shigellosis is a common food-borne disease that causes approximately 125 million episodes of shigellosis in the Asian countries and claims more than 1.1 million deaths per year throughout the world [1, 2]. The family of Enterobacteriaceae includes the gram-negative, facultative anaerobic bacilli, non-sporulating bacteria-*Shigella flexneri*, which is spread via food, houseflies with high infective dose and sometimes sexual contact with lower [1, 3, 4].

Shigella infection site is mainly the large intestine, where the epithelial cell is the specific hosting cell. Multistep process of *Shigella flexneri* invasion starts with the entry of bacteria into the M (micro-fold)-cell and then epithelial cell [5]. For entrance, *Shigella* uses the type three secretion system, a needle like hollow tube which is 50nm long and 7nm thick and made of MxiH protein's helical assembly [6], which is used for the translocation of effector-translocator proteins, ipaB and ipaC that are secreted and chaperoned into the bacterial cytoplasm. These proteins are mainly required for the entry of bacteria into the host cell following the physical contact with a host cell, forming a complex together and their step-wise association is required to form the pore on lipid bilayer of host cell membrane [7-9]. Though the ipaB is essential to cause the host cell death after proper insertion into host cell, which is mediated by caspase-1, an enzyme found in human [10], but ipaB and ipaC both are chaperoned by ipgC which is important for stability of these two major invasins [11]. There are many important effector proteins but the main target of this study is invasion protein antigen D (ipaD), located at the needle tip of the type three-secretion system with mxiH through its C-terminal residues. The ipaD is essential for secretion control and proper insertion of translocators into host cell membranes from bacterial cytoplasm [12]. Virulence process of *Shigella flexneri* is the ability of ipaD to localize to the TTSA needle tip and recruit ipaB to the surface after appropriate signal detection from environment. No ipaB recruitment occur when the conformation of ipaD changes results in less affinity to deoxycholate, a bile salt in small intestine [13]. By

acting as a plug to the T3SA, ipaD is a protein to prevent the attachment of bacteria with target cell to stop the invasion by transferring effector proteins into the host cell [14]. The ipaB protein attaches with the ipaD to be trancytosed from bacterial cytosol to host cell after stable attachment with of ipaD with mxiH at needle tip of T3SA [15]. The ipaD is attached with mxiH with its C-terminal residues, Asn40, Ser42, Asn43 and Glu45 which forms a PSPN loop all together and the N-terminal domain extends the needle [16]. The drug target of shigellosis using N-terminal domain of ipaD can be potential target, [17] as there is a priority of vaccine development of *Shigella flexneri* as well shigellosis [1].

Though it is proved that bile salt induce the ipaB recruitment at needle tip with ipaD [15] but in large intestine, there is very small amount of bile salt that is excreted through feces from human body. Therefore, bile salt binding site is another site of ipaD inhibition; it can be, this is another binding site for ligand, which is a different molecule than deoxycholate. Through these two ways, conformational change can be an outcome of ligand binding on the active site of ipaD-can prevent shigellosis-targeting ipaD for preventing ipaB being attached at the needle tip.

MATERIALS AND METHODS

The sequence of the target protein, invasion protein antigen, ipaD of *Shigella flexneri* was retrieved from UniProt (Universal Protein Resource) and the accession number of the protein is P18013 of 332 amino acid residues.

The similarity search of ipaD was done with BLASTp (Basic Local Alignment Search Tool for protein) [18] against Protein databank (PDB) [19]. The model of ipaD was generated using Modeller (version 9.10) [20]. interactive modeling with high level of identity. The templates were 3R9V and 2J0N.

The verification of the structure and the quality were estimated using the PROCHECK [21], VERIFY3D [22] and ERRAT [23] at Structural Analysis and Verification Server (SAVES, Version 3). Ligand binding pocket was find out using Computed Atlas of Surface Topography of proteins (CASTp) [24] and the pocket visualization to determine the pocket center using the CASTp plugin of Pymol.

The ligands were collected from the ZINC database [25] and spitted and prepared for docking using Raccoon [26]. To carry out the the protein ligand interaction, AutoDockVina was used as docking tool, as it is used for the flexible ligand docking with protein using Lamarckian Genetic Algorithm (LGA) method [27]. Using the MGL tools version1.5.7 used to add polar hydrogen atom to the modelled ipaD and to generate suitable format for docking. Protein structure visualization was done using Pymol and bonds between compounds of ligands and ipaD were analyzed using Discovery Studio3.5.

RESULTS AND DISCUSSION

The two best similar sequences from BLASTp result (Table 1) were taken as template for modeling of target protein sequence, based on the identity, e-value and the query coverage.

Table 1. The BLASTp result of target protein sequence against PDB

Accession Number of Template	Query Coverage	E-value	Total Score	Maximum Score	Identity
PDB: 2J0O	95%	0.0	648	648	99%
PDB: 3R9V	95%	0.0	579	579	99%

Protein modeling was done using computer based tool-Modeller 9.10 and ten models were built from these, best model was selected with lowest DOPE (Discrete Optimized Protein Energy) score.

After homology modeling, the stereo-chemical properties of modelled protein analysis show that the favorable region of Ramachandran plot is 92.2% where 283 amino acids are favored among 332. The ERRAT quality factor is 88.294 shown in figure 1. A good model quality shows, as the Z-score RMS should be near to one. The built model shows 2 small alpha helices, 2 medium sized and 4 long alpha helices where 4th and 5th helices are attached with two beta sheet, 6th and 7th, the two small helices have more two sheet between them and 7th and 8th have another one between them.

From CASTp calculation, first three pockets were considered based on their volume. The pocket 44 has the area 340.2 Å2 with the volume of 843.2 Å3 respectively. Moreover, the pocket 43 contains 330.3 Å2 area with 570.4 Å3 volume, and pocket 42 has 384.3Å3 volume and 300.5Å2 area (figure 2).

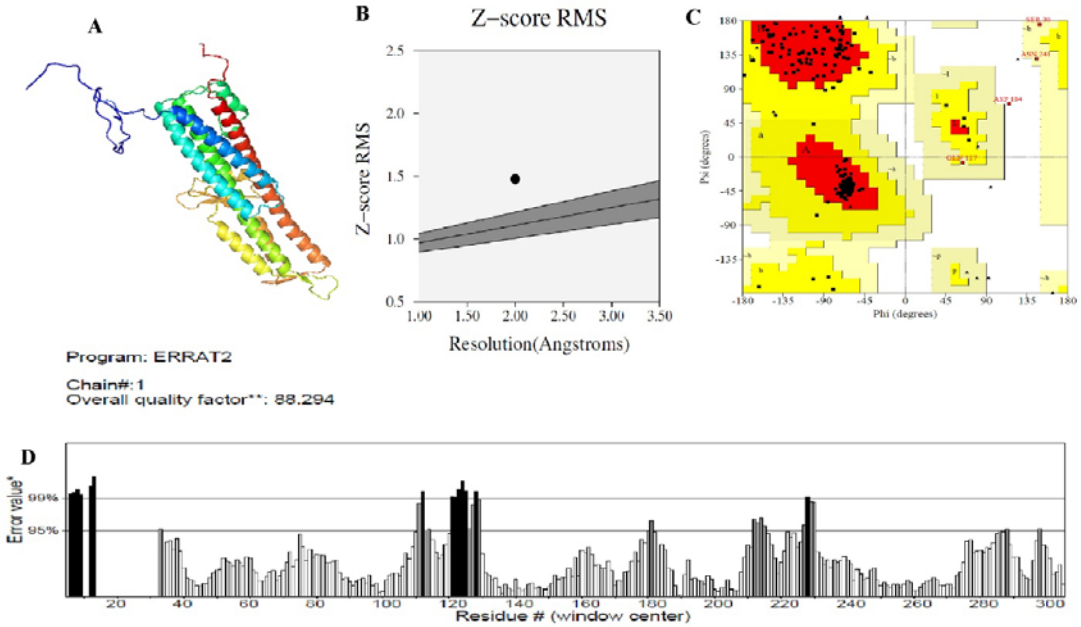

Figure 1. The ipaD structure based on two template, secondary structure of the model is in figure A. Figure B shows the stereochemical properties of modelled protein from Ramachandran plot. Ramachandran Plot of modelled protein and in four angles the amino acids are shown in colors, here, allowed amino acids are shown in yellow color and red is the most allowed amino acids in figure C. In D, the Z-score RMS is 1.476 of the model and the ERRAT quality factor is 88.294.

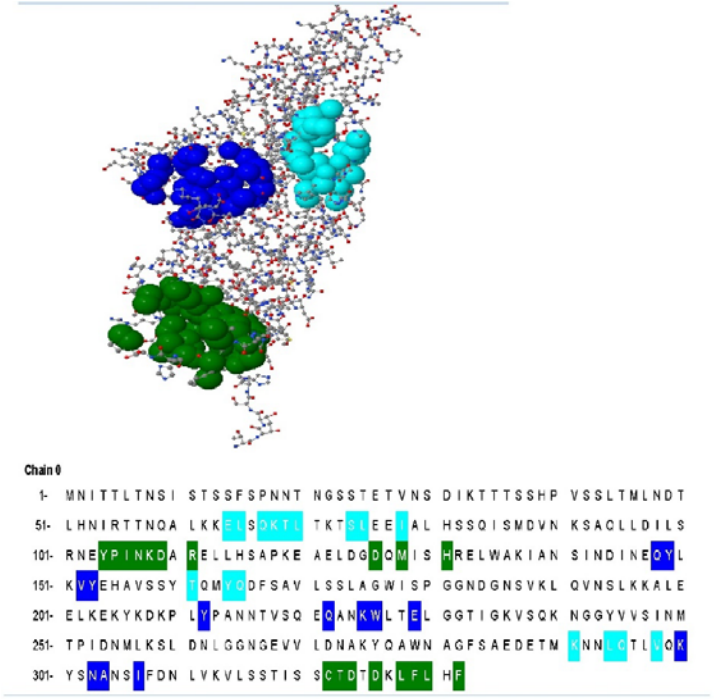

Figure 2. Three pockets are showing in colors in a wireframe display of ipaD. Pockets are showing in spheres of for 44, 43 and 42 in green, dark blue and sky blue color respectively. The table shows pockets forms by respective amino acids.

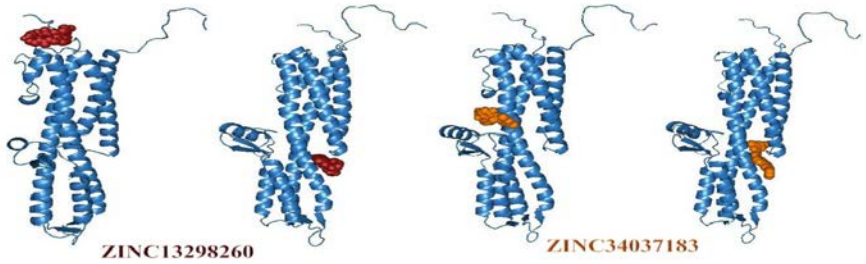

Figure 3. Brick red showing the binding of ZINC13298260 at two different sites of the modelled protein ipaD. ZINC34037183 also binds at two different sites. Three hydrogen bonds found between ZINC34037183:H13-TYR212:OH with length of 2.39821 Å, ZINC34037183:H9-GLU147:O where length is 2.13563 Å and ZINC34037183:H1-TYR149:OH with 2.48097Å with ipaD(not shown).

Table 1. Summary of ipaD and ligand docking with respect to the binding pocket

Pocket	ZINC Database Id	Chemical name	Binding affinity(kj/mol)
44	ZINC13298260	Lunarine	-9.1
	ZINC90398243	3- 4-(2,6-dimethylphenyl)-1-piperidyl methyl -1,2-diphenyl-indole	-8.6
	ZINC61389490	7-DESACETOXY-6,7-DEHYDROGEDUNIN	-8.5
	ZINC03978112	Dihydrogedunin	-8.5
	ZINC03978266	1,7-dideacetoxy-1,7-dioxo-3-deacetylkhivorin	-8.4
43	ZINC34037183	N- 2-fluoro-5- 3- (E)-2-pyridin-2-ylethenyl -1H-indazol-6-yl amino phenyl -2,5-dimethylpyrazole-3-carboxamide	-9.6
	ZINC90594098	3- 3- 4-(trifluoromethyl)-1,3-benzothiazol-2-yl oxy azetidine-1-carbonyl chromen-2-one	-9.2
	ZINC06404575	N-(1-benzyl-2-hydroxy-indol-3-yl)imino-4-methyl-benzenesulfonamide	-9.1
	ZINC90398225	2- 4-(2,6-dimethylphenyl)-1-piperidyl methyl -3-phenyl-1H-indole	-9.0
	ZINC90479805	1-(3-cyano-4-fluoro-phenyl)-3- 3-(5-methyl-4H-1,2,4-triazol-3-yl)phenyl methyl urea	-8.7
42	ZINC13298260	Lunarine	-9.9
	ZINC34037183	N- 2-fluoro-5- 3- (E)-2-pyridin-2-ylethenyl -1H-indazol-6-yl amino phenyl -2,5-dimethylpyrazole-3-carboxamide	-9.8
	ZINC20148998	BMS-1 or 1-(4-fluorophenyl)-N- 3-fluoro-4-(1H-pyrrolo 2,3-b pyridin-4-yloxy)phenyl -2-oxo-1,2-dihydropyridine-3-carboxamide	-9.5
	ZINC90479705	1- (2R)-2-(4-fluorophenyl)-2-hydroxy-propyl -3- 3-(5-methyl-1H-1,2,4-triazol-3-yl)phenyl urea	-9.4
	ZINC90459839	(1R,2R)-N- (3R,9aR)-1,3,4,6,7,8,9,9a-octahydropyrido 2,1-c 1,4 oxazin-3-yl methyl -2-(1-naphthyl)c	-9.4

Three best pockets were selected for docking, using the CASTp plugin for Pymol the grid box were calculated for free ligand rotation. The grid box size for pocket 44 was 27×26×25, for pocket 43, 24×26×21, and pocket 42, 23×19×26. The docking was performed using AutoDock Vina and the result shows the binding affinity in kj/mole. The best docking result which is the lowest binding energy where RMSD is zero, from possible 10 conformation of ligand binding to ipaD. Table 2 shows five best ligand from ZINC database for three different pockets with their binding free energy. The lowest free binding energy shows the ligand quality to be attached with the protein. The selected ligands are considered because of their good binding free energy and RMSD value.

The physicochemical properties of selected ligands that consider for the Lipinski rule are shown in table 3. Properties are collected from the physical representation of compound in ZINC database.

Table 2. Lipinski properties of the selected ligands

No.	ZINC database ID	MW	HBD	HBA	RB	xLogP	TPSA
1	ZINC13298260	438.548	4	7	0	1.22	101
2	ZINC90398243	471.668	1	2	5	7.70	9
3	ZINC61389490	422.521	0	5	1	4.05	69
4	ZINC03978112	484.589	0	7	3	4.36	95
5	ZINC03978266	456.535	1	7	1	2.56	106
6	ZINC34037183	465.508	3	8	6	4.75	101
7	ZINC90594098	446.406	0	6	4	3.84	73
8	ZINC06404575	404.471	0	6	5	4.32	83
9	ZINC90398225	395.57	2	2	4	6.72	20
10	ZINC90479805	350.357	3	7	4	2.32	106
11	ZINC20148998	458.424	2	7	5	4.03	89
12	ZINC90479705	369.4	7	4	5	2.639	102.928
13	ZINC90459839	365.495	2	4	4	3.54	43

MW=molecular weight, HBD=hydrogen bond donor, HBA=hydrogen bond acceptor, RB= rotatable bond, TPSA= topological polar surface area, XlogP: as a predictor for LogP in quantitative structure activity relationship (QSAR study).

CONCLUSION

Molecular docking studies performed against a dataset of total 14933 compound from ZINC database. From the docking result, first ligand (ZINC13298260) attached with alpha4, alpha6 and alpha8 helices, where interaction at the interface between alpha2 and alpha8 helix also found. Another ligand have the lowest free energy at two different sites of ipaD is the sixth ligand (ZINC34037183) showing similar binding affinity at the interface between alpha4, alpha6 and alpha8 helices. This ligand also bound at the interface between alpha2 and alpha8 with lowest binding energy than before. From this study, 13 ligands showing low binding energy at three different sites of ipaD but ZINC13298260 and ZINC34037183 are the best ligands for their low binding affinity at multiple sites of ipaD shown in figure 3.

All ligands are known to be Lipinski compliant. Therefore, it can be concluded that these ligands can be ipaD inhibitors, with optimum binding affinity and drug-like properties. This theorized study shows a set of good ligands for inhibition of ipaB recruitment at needle tip, after binding with the ipaD, so that it cannot create a pore along with ipaC or binding at alpha8 helix near the active site of ipaD prevent the protein from binding with mxiH at needle tip. Further the bioavailability and ADMET testing is suggested for the acceptability of these ligands as drug.

Acknowledgements

Our acknowledgement to the department of Computer Science and Engineering, Shahjalal University of Science and Technology for their laboratory assistance.

REFERENCES

1. Niyogi SK (2005). Shigellosis. J Microbiol. 43:133-43
2. Bardhan P, Faruque AS, Naheed A et al. (2010). Decrease in shigellosis-related deaths without Shigella spp.-specific interventions, Asia. Emerg Infect Dis. 16:1718-23.
3. Farag TH, Faruque AS, Wu Y et al. (2013). Housefly Population Density Correlates with Shigellosis among Children in Mirzapur, Bangladesh: A Time Series Analysis. PLoS Negl Trop Dis. 7: e2280.
4. Viroj Wiwanitkit MD (2006). Sexually transmitted shigellosis. Sexuality and Disability. 24:69-71.
5. Schroeder GN and Hilbi H (2008). Molecular pathogenesis of Shigella spp.: controlling host cell signaling, invasion, and death by type III secretion. Clin Microbiol Rev. 21:134-56.
6. Fujii T, Cheung M, Blanco A, Kato T et al. (2012). Structure of a type III secretion needle at 7-A resolution provides insights into its assembly and signaling mechanisms. Proc Natl Acad Sci U S A. 109: 4461-6.
7. Blocker A, Gounon P, Larquet E, Niebuhr K et al. (1999) The tripartite type III secreton of Shigella flexneri inserts IpaB and IpaC into host membranes. J Cell Biol. 147: 683-93.
8. Roehrich AD, Guillossou E, Blocker AJ et al. (2013) Shigella IpaD has a dual role: signal transduction from the type III secretion system needle tip and intracellular secretion regulation. Mol Microbiol. 87:690-706.
9. Picking RDMEMDLWD (1998). Protein-protein interactions in the assembly of Shigella flexneri invasion plasmid antigens IpaB and IpaC into protein complexes. Biochim Biophys Acta. 1429: 45-56.
10. Zychlinsky A, Prevost MC and Sansonetti PJ (1992). Shigella flexneri induces apoptosis in infected macrophages. Nature. 358 :167-169.
11. Vasselon RMPSCPT (1994). Extracellular association and cytoplasmic partitioning of the IpaB and IpaC invasins of S. flexneri. Cell. 79: 515-25.
12. Espina M, Olive AJ, Kenjale R et al. (2006) IpaD localizes to the tip of the type III secretion system needle of Shigella flexneri. Infect Immun. 74: 4391-400.
13. Stensrud KF, Adam PR, La Mar CD et al. (2008) Deoxycholate Interacts with IpaD of Shigella flexneri in Inducing the Recruitment of IpaB to the Type III Secretion Apparatus Needle Tip. Journal of Biological Chemistry. 283: 18646-18654.
14. Sani M, Botteaux A, Parsot C et al. (2007) IpaD is localized at the tip of the Shigella flexneri type III secretion apparatus. Biochimica et Biophysica Acta (BBA) - General Subjects. 1770: 307-311.
15. Olive AJ, Kenjale R, Espina M et al. (2007) Bile salts stimulate recruitment of IpaB to the Shigella flexneri surface, where it colocalizes with IpaD at the tip of the type III secretion needle. Infect Immun. 75: 2626-9.
16. Zhang L, Wang Y, Olive AJ et al. (2007) Identification of the MxiH needle protein residues responsible for anchoring invasion plasmid antigen D to the type III secretion needle tip. J Biol Chem. 282: 32144-51.
17. Epler CR, Dickenson NE, Bullitt E et al. (2012) Ultrastructural analysis of IpaD at the tip of the nascent MxiH type III secretion apparatus of Shigella flexneri. J Mol Biol. 420: 29-39.
18. Altschul SF, Gish W, Miller W et al. (1990) Basic local alignment search tool. J Mol Biol. 215: 403-10.
19. Bourne PE, Addess KJ, Bluhm WF et al. (2004) The distribution and query systems of the RCSB Protein Data Bank. Nucleic Acids Res. 32: D223-5.
20. Narayanan Eswar BW, Marc A Marti-Renom, Madhusudhan MS (2006). Comparative protein structure modeling using Modeller. Curr Protoc Bioinformatics. Chapter 5: Unit 5 6.
21. Laskowski RA, MacArthur MW, Moss DS et al. (1993) PROCHECK: a program to check the stereochemical quality of protein structures. Journal of Applied Crystallography. 26: 283-291.
22. Luthy R, Bowie JU, Eisenberg D (1992). Assessment of protein models with three-dimensional profiles. Nature. 356: 83-85.
23. Colovos, C and Yeates TO (1993). Verification of protein structures: patterns of nonbonded atomic interactions. Protein Sci. 2:1511-9.
24. Dundas J, Ouyang Z, Tseng J et al. (2006) CASTp: computed atlas of surface topography of proteins with structural and topographical mapping of functionally annotated residues. Nucleic Acids Res. 34(Web Server issue): W116-8.
25. Irwin, JJ and Shoichet BK (2004). ZINC – A Free Database of Commercially Available Compounds for Virtual Screening. J. of Chemical Information and Modeling. 45: 177-182.
26. Cosconati S, Forli S, Perryman AL et al. (2010) Virtual Screening with AutoDock: Theory and Practice. Expert Opin Drug Discov. 5: 597-607.
27. Trott O, Olson AJ (2010). AutoDock Vina: improving the speed and accuracy of docking with a new scoring function, efficient optimization, and multithreading. J Comput Chem. 31: 455-61.

*****